PERFORMANCE OF A REINFORCED EARTH FILL

Jerry C. Chang, Raymond A. Forsyth, and John L. Beaton,
California Department of Transportation

Design methods and field performance studies are presented for the reinforced earth embankment on Cal-39 in Los Angeles County. Rankine's state of stress theory was employed to derive the equations for designing the reinforcement. Strain energy principle was introduced to develop the equations for designing the steel skin plate. Comprehensive instrumentation was installed to study the field behavior. The field-observed data indicate close agreement between the design assumptions and field behavior. Recommendations concerning stability analyses and corrosion were also included.

•REINFORCED earth is soil mass composed of fill strengthened by metal or plastic reinforcements and enclosed at the front face by skin elements. Since at least Roman times, builders have been aware of the stabilizing effect of including reinforcing elements in earthwork. In his commentaries, Julius Caesar (1) stated

> All Gallic walls are commonly of this fashion: straight beams are laid together upon the ground at equal intervals of two feet, their inner ends braced together, while along the outer front the interspaces are packed with large blocks of stone, and the whole is covered with earth. Upon these is laid a second similar row of beams, so that while the same interval is maintained, the beams of the two rows are not contiguous. . . .In this way the whole wall is built up course by course until the full height is maintained.

The beams described were to reinforce the earth with a stone outer face to resist impact or battering. The use of earthwork reinforcement based on rational design was reported in 1969 by Henri Vidal (2). In October 1972, the first application of reinforced earth to highway construction in the United States was carried out by the California Department of Transportation to reopen a section of Cal-39 in the San Gabriel Mountains, Los Angeles County, that had been closed by a surficial debris slide during a heavy spring storm in 1969. A description of the slide and the rationale for selecting reinforced earth for its correction were reported by Chang, Forsyth, and Smith (3) in 1972. They also presented the results of soil investigation and stability analysis and equations developed for analyzing the stresses in the reinforcing strips. By using these equations, the size, length, and spacings of the suggested reinforcement were evaluated.

In this paper, equations for analyzing the stresses in the skin plates, comparisons between the field instrumentation data, and analytical results for both reinforcing strips and skin plates are presented. Results of field pulling tests on the reinforcement are included also.

EMBANKMENT GEOMETRY

The reinforced earth fill was constructed on top of a random fill embankment founded over the slide debris. At the bottom of the slide debris a toe buttress was built to act as a stabilizing fill embankment. The overall height of the system was approximately 360 ft. The reinforced earth fill had a maximum height of 55 ft and length of 528 ft.

Publication of this paper sponsored by Committee on Embankments and Earth Slopes.

Figure 1. Plan and profile.

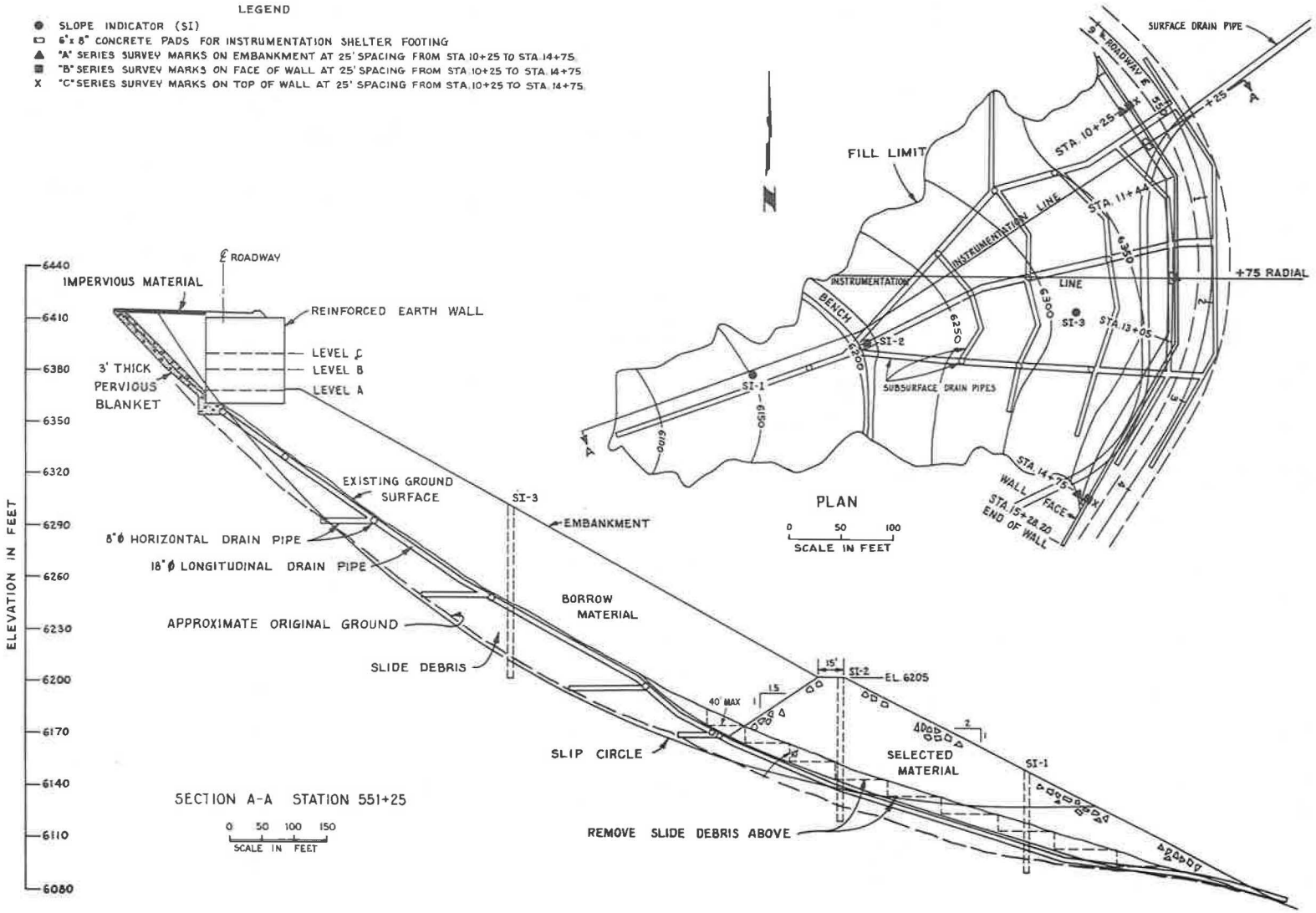

A system of surface and subsurface drain pipes was installed to remove surface water and seepage. The embankment is shown in plan and profile in Figure 1.

DESIGN OF REINFORCEMENT

The 2 basic equations for analyzing the reinforcement design were based on Rankine's state of stress theory and the principles shown in Figures 2 and 3. The equations were developed as follows assuming a Rankine's active earth pressure, p, acts on the inner face of the skin plate (3):

$$p = K_a \gamma H$$

where

K_a = coefficient of active earth pressure,
γ = unit weight of soil, and
H = height of fill.

A force, T, will be developed in the reinforcing strip, and it tends to either pull the strip out or fail it in tension. The pull force, T, and the stress, f_s, developed in the strip will be

$$T = K_a \gamma H d \Delta H \tag{1}$$

$$f_s = \frac{K_a \gamma H d \Delta H}{bt} \tag{2}$$

where

d = horizontal spacing of strips,
ΔH = vertical spacing of strips,
b = width of steel strip, and
t = thickness of steel strip.

Figure 2. Schematic of reinforced earth fill.

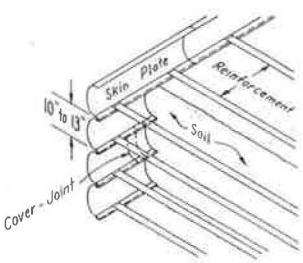

Figure 3. Schematic of reinforced earth block.

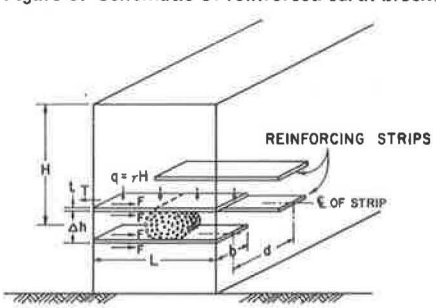

Let the skin-friction angle be ϕ_u. A friction force, F, will be developed on each face of the strip so that

$$F = \gamma H b L \tan\phi_u \tag{3}$$

The factor of safety against slippage, S.F., will be

$$S.F. = \frac{2F}{T} = \frac{2\gamma H b L \tan\phi_u}{K_a \gamma H d \Delta H} = \frac{2bL\tan\phi_u}{K_a d \Delta H} \tag{4}$$

Equation 2 was used to compute theoretical steel stresses for comparison to those measured by field instrumentation.

DESIGN OF SKIN PLATES

The standard shape of the skin plate consisted of a semielliptical element 10 to 13 in. high with a thickness of about $\frac{1}{8}$ in.

To simplify the stress analysis, the following assumptions were made for a semicircular section of skin plate: (a) the soil pressure distribution and deformation

Figure 4. Loading diagram on skin plate.

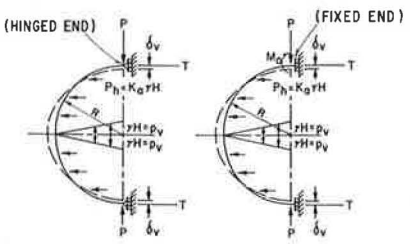

configuration as shown by Figure 4 and (b) that a vertical load, P, representing a resultant force transferred from a uniform vertical pressure acting along an effective length of reinforcing strip will cause a vertical deformation, δ_v. This vertical deformation was assumed to have the same magnitude as the settlement of the soil mass caused by a uniform vertical soil pressure acting on the top and bottom row of reinforcement.

By using strain energy principles described by Seely and Smith (5), the equations for computing the vertical load, P, and the end moment, M_a, were developed as follows (4): For hinged-end conditions as shown in Figure 4

$$P = \frac{4EI\delta_v}{R^3\pi} - \frac{4K_a\gamma HR}{3\pi} - \frac{\gamma HR}{24\pi}(3\pi - 32) \tag{5}$$

and for fixed-end conditions

$$P = \frac{\delta_v EI}{\pi R^3}\left(4 - \frac{32}{8 - \pi^2}\right) + \gamma HR\left(\frac{4 - 4K_a}{3\pi} - \frac{1}{8}\right) - \frac{8\gamma HR}{8 - \pi^2}\left[\frac{4 - 4K_a}{3\pi} - \frac{(1 + \pi - \pi K_a)}{8} + \frac{1}{9}\right] \tag{6}$$

and

$$M_a = \frac{8\delta_v EI}{R^2(8 - \pi^2)} + \frac{2\pi\gamma HR^2}{(8 - \pi^2)}\left[\frac{4 - 4K_a}{3\pi} - \frac{(1 + \pi - \pi K_a)}{8} + \frac{1}{9}\right] \tag{7}$$

The magnitude of P depends on the restraint conditions at the ends and the value of vertical settlement, δ_v. When the unknown load, P, and the unknown bending moment, M_a (Fig. 4), are determined, the stresses developed in the skin plate can be calculated. Equations 5, 6, and 7 can be solved by measuring the vertical deformations, δ_v, in field performance studies or laboratory scale model tests. For design purposes, a value of δ_v can be determined by estimating the embankment settlement.

CONSTRUCTION MATERIAL

Triaxial tests (consolidated drained condition) on the backfill material resulted in a friction angle, ϕ, of 40 deg at 95 percent relative compaction. From this, Rankine's coefficient of active earth pressure, K_a, was calculated to be 0.22. The coefficient of earth pressure at rest, K_o, was computed to be 0.36 based on Jaky's expression (6), $K_o = 1 - \sin\phi$. Laboratory skin friction tests between the galvanized steel strip and the soil resulted in a skin-friction angle of 31 deg.

The dimensions of the steel reinforcing strips were as follows:

1. Thickness: 0.118 in.,
2. Width: 2.362 in., and
3. Length: 22.79 to 46.0 ft.

Laboratory tests resulted in a yield strength of 37,000 psi; an ultimate strength of 40,000 psi; a Young's modulus of 28.5×10^6 psi; and a Poisson's ratio of 0.28.

INSTRUMENTATION

To monitor the behavior of the completed structure, comprehensive instrumentation

was installed in the field. Included were

1. Slope indicators to measure internal deformation of the embankment and slide debris;
2. Settlement platforms to measure vertical settlements;
3. Extensometers to measure soil strains;
4. Soil pressure cells to measure soil stresses;
5. Strain gauges to measure stresses developed in the reinforcing strips and skin plates; and
6. Gauge points to measure deformations of the skin plates and the wall face. Locations of the instruments are shown in Figures 1 and 5. All instruments were read periodically during construction and for approximately 1 year after completion of the embankment.

STRESSES IN THE REINFORCING STRIPS

The daily history of the axial stresses in the steel strips is shown in Figure 6. They were calculated based on average strain recorded on top and bottom of the strip and a modulus of elasticity of 28.5×10^6 psi. For comparison, steel stresses assuming active earth pressure and at rest cases were computed by using Eq. 2 superimposed on Figure 6. The lowest axial stresses were measured near the wall face. After completing the fill, the stresses near the wall face decreased with time and eventually became compressive at level A. This phenomenon probably was due to the restraint provided by the berm. At 15 and 25 ft from the wall face, the stresses in the strips increased with time and finally reached the calculated stress, σ_a, based on coefficient of active pressure, K_a. At level B, the steel stresses at 15 ft from the wall face decreased with time to values much lower than σ_a; the stresses at 25 ft from the wall face increased with time and approached the calculated stress, σ_o, based on coefficient of earth pressure at rest, K_o. At level C, the magnitude of all steel stresses decreased with time and approached σ_a.

SOIL STRESSES

Figure 7 shows the soil stresses measured at section III, station 551+75. The ratio, K, between the horizontal stress and vertical stress is also plotted on this figure. The γH lines represent the theoretical vertical soil stresses computed by using a unit weight, γ, of 143 pcf and the corresponding depth of fill, H, over each instrumentation level. The K values varied irregularly during and immediately after construction presumably because of the effect of compaction. As the height of fill increased over the instrumentation level, the influence of compaction diminished. After completion of the fill, the K values still varied between 0.5 and 0.8 at this section as compared to the calculated K_a of 0.22 and K_o of 0.36. At the other sections (not shown) the K values varied from 0.11 to 0.41.

STRESSES IN THE SKIN ELEMENTS

Figure 8 shows the daily history of stresses in the skin element. The locations and the identification numbers of the strain gauges are shown on top of the figure. Gauges 1, 5, and 9 measured axial strain on the outside of the face; gauges 3, 7, and 11 measured axial strains on the inside. Gauges 2, 6, and 10 measured circumferential strain on the outside of the face; gauges 4, 8, and 12 measured circumferential strain on the inside. The actual deformation of the skin elements closely approximated the deformation assumed in developing Eqs. 3, 4, and 5. Accordingly, tensile circumferential stresses developed on the outside of the face, and compressive circumferential stresses developed on the inside. Deformations of the skin elements were measured at 5 gauge points on the faces of the skin plates with a specially designed vernier-micrometer caliper capable of accurately measuring to 0.001 in. The measured relationship between the vertical deformation of the skin plate and fill height is shown in Figure 9. Based on the vertical deformations observed in the field, the stresses in the skin plates were calculated for both hinged- and fixed-end conditions. A comparison of the measured and com-

Figure 5. Instrumentation sections.

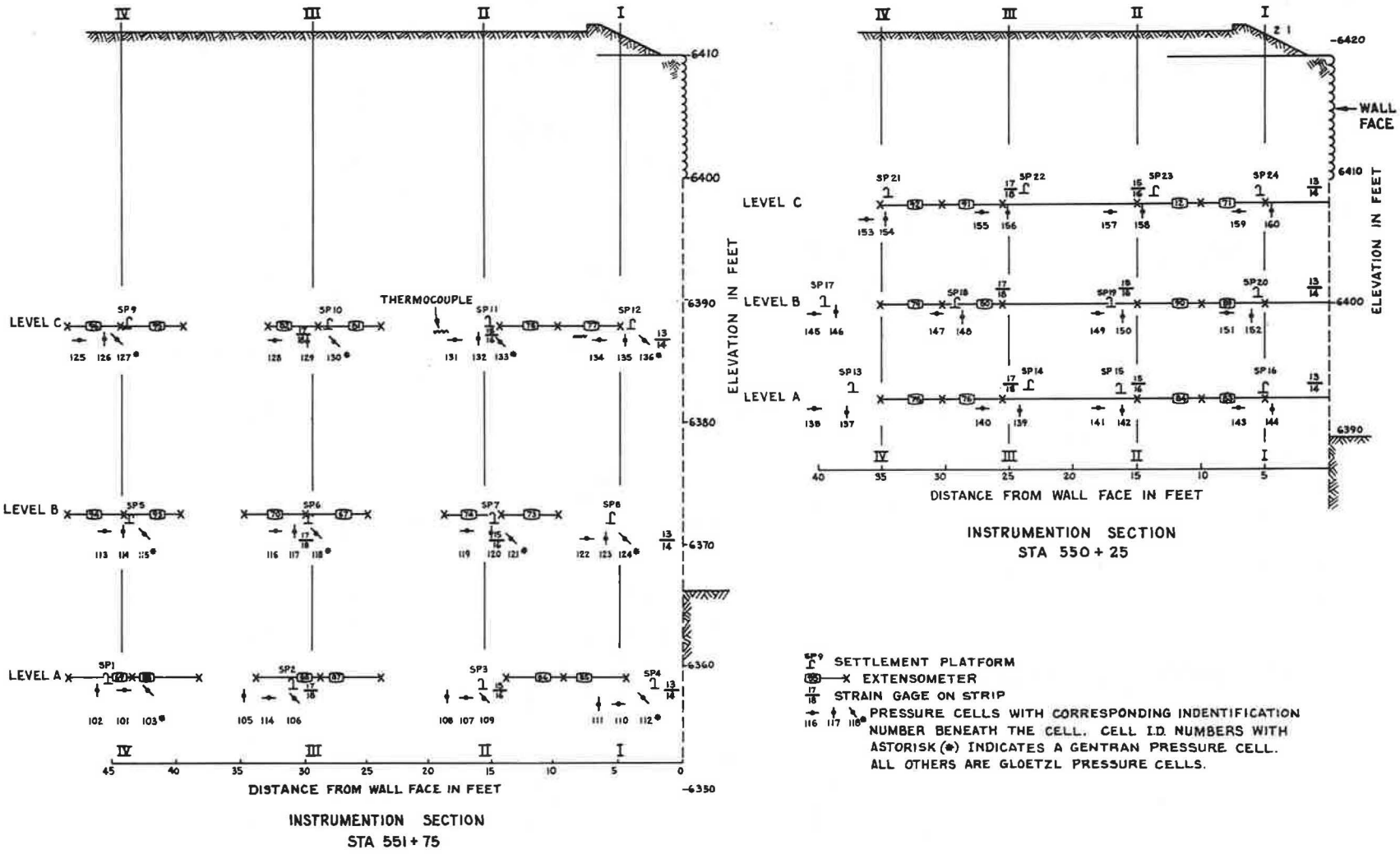

Figure 6. Daily history of stresses in steel strip.

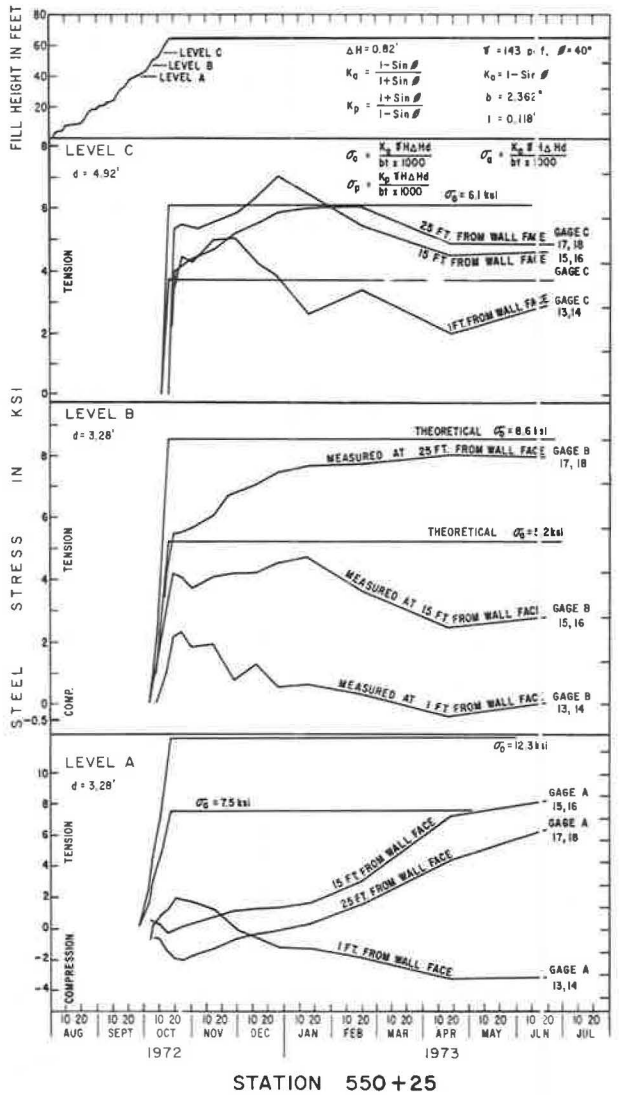

STATION 550+25

Figure 7. Daily history of soil stress.

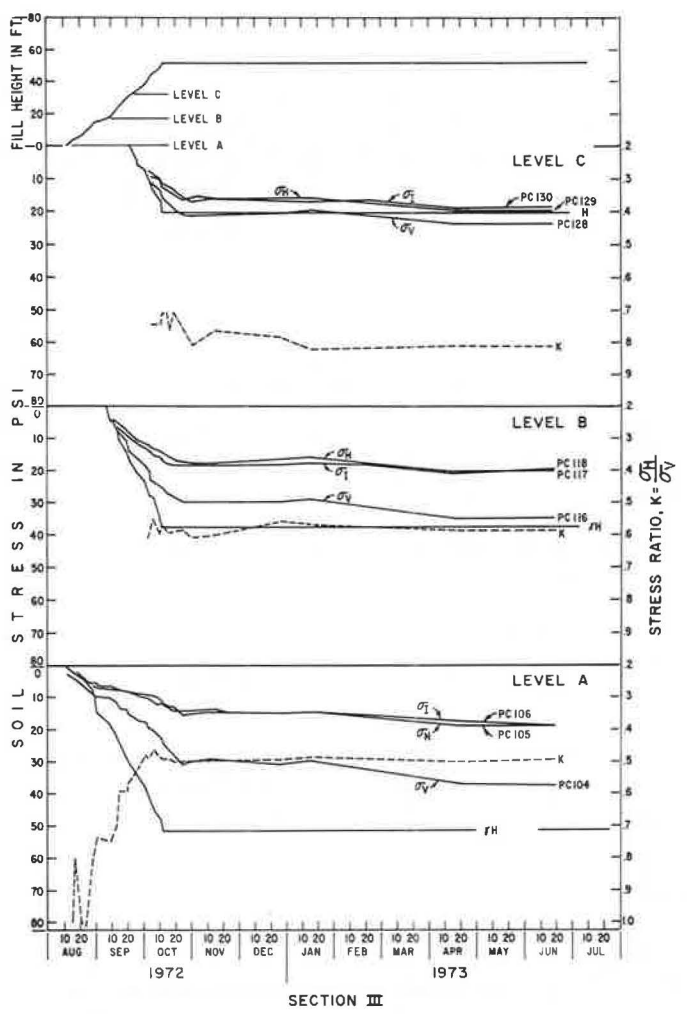

SECTION III

Figure 8. Daily history of stress in skin element.

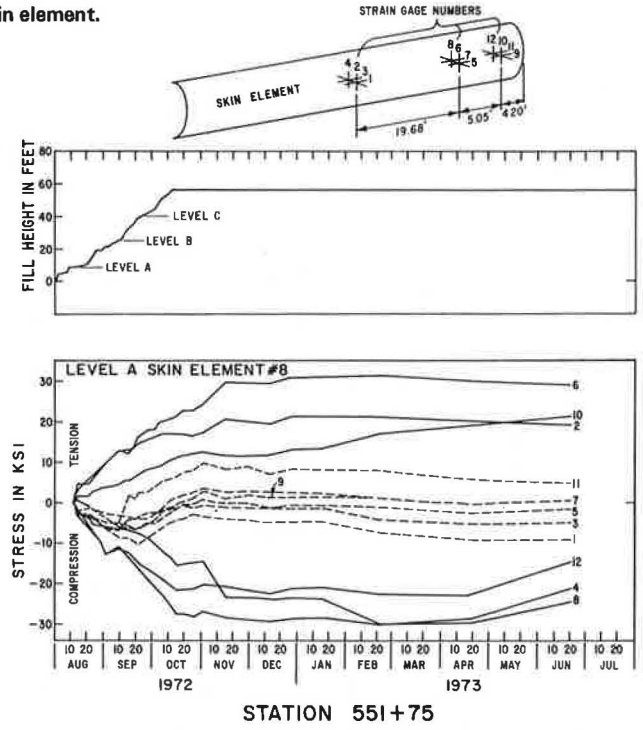

Figure 9. Field behavior of steel skin element.

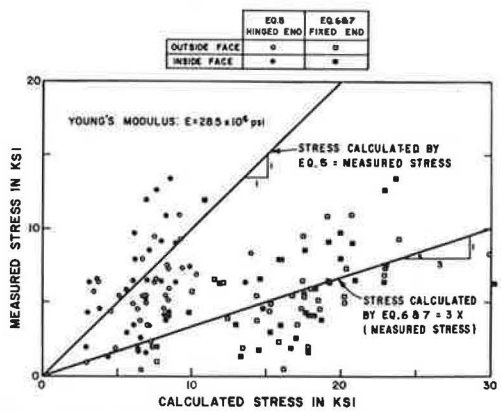

(a) COMPARISON OF MEASURED AND CALCULATED CIRCUMFERENTIAL STRESS AT SPRING LINE OF SKIN PLATE

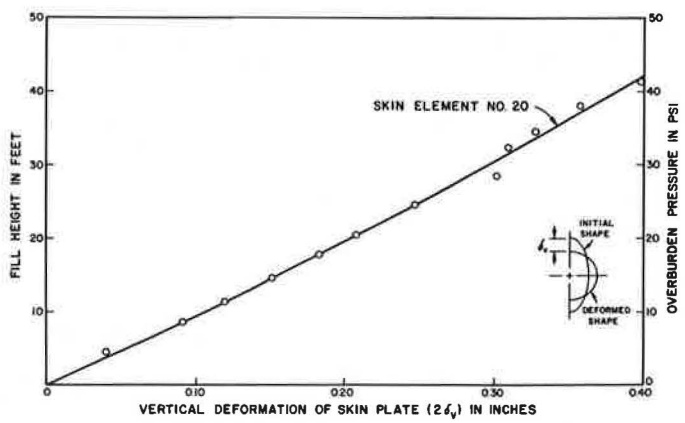

(b) RELATIONSHIP BETWEEN FILL HEIGHT AND SKIN PLATE DEFORMATION STATION 551+75

puted circumferential stresses also is shown in Figure 9. The calculated stresses based on hinged-end assumption (Eq. 5) agreed reasonably well with the measured data although the calculated stresses based on the fixed-end condition (Eqs. 6 and 7) were almost 3 times larger than those measured.

FIELD PULLING TESTS

To test the validity of Eqs. 3 and 4, dummy reinforcing strips were installed in the fill at 5 levels for field pulling tests. Three strips, 5, 10, and 15 ft in length, were embedded at each of 3 levels under overburden heights of 7.5, 12.4, and 18.2 ft. Three 23-ft strips were embedded at a depth of 18 ft; three 46-ft strips were embedded at a depth of 38 ft. One of the 23-ft strips and 1 of the 46-ft strips were instrumented with strain gauges on both top and bottom at 5-ft intervals.

A typical load deformation curve obtained from field pulling tests is shown in Figure 10 for a 5-ft strip. Three pulling loads were defined for analysis and indicated on the curves. These were

1. Yield loads representing the proportional limit of the load-deformation relationship,
2. Peak load representing the maximum pulling load, and
3. Residual load representing the pulling load when deformation increases appreciably without a change in the pulling load.

Figure 11 shows the relationships between the residual pulling load, overburden load, overburden height, and strip length. The skin-friction angles, ϕ_u, of 31 deg obtained from the residual pulling load plots agreed well with the laboratory test results at equal overburden pressure. For a constant overburden height, the residual loads were proportional to the overburden loads, which are the products of the overburden height, H; the unit weight, γ; the width of steel strip, b; and the length of the steel strip, L. Because γ, b, and H are constant under a given overburden height, the residual loads are proportional to the strip length. Because the peak load represents the maximum mobilized friction grip, it was used to calculate the factor of safety for the failure condition. The design tensile loads were calculated by using Eq. 1. The relationships between overburden height, H, strip length, L, and slipping factor of safety are shown in Figure 12. For a fill height of 10 ft, the minimum strip length may require only 9 ft for a factor of safety of 4. Figure 13 shows the relationship between peak pull load and the calculated skin-friction force (3). Peak pull loads exceeded the skin-friction force as the strip length exceeded 10 ft. We may conclude that strip length should be at least 10 ft.

AXIAL FORCES IN DUMMY STRIPS BECAUSE OF STATIC LOADING

Figure 14 shows the relationship between overburden loads and the maximum axial force observed in the 46-ft and the 23-ft strips at 10 to 15 ft from the wall face. The axial forces developed during construction were all lower than the calculated tensile force, T_a, from Eq. 1 based on the Rankine's active earth pressure coefficient, K_a. However, after the fill was completed the axial force continued to increase and the maximum axial force reached T_a in the 23-ft strip. In the 46-ft strip, the maximum axial force finally reached T_o, the calculated tensile force from Eq. 1, based on the at rest earth pressure coefficient, K_o. The continuous increase in tensile force after completion of the fill probably was due to the continuing settlement. At completion of construction and 8 months later, the settlements on levels B and C, station 551+75, varied from 1.5 to 2.5 ft. However, on level A, the settlement varied from 2.5 to 3.5 ft. Also, the face of the wall has moved a maximum of 0.7 ft horizontally downslope since completion of the fill. Both horizontal movement and settlement are attributed primarily to densification of the uncompacted slide debris.

SUMMARY AND CONCLUSIONS

The measured vertical soil stresses generally agreed with the calculated vertical earth pressures. The stress ratios, K, between the horizontal and vertical soil stresses

Figure 10. Typical load deformation curve.

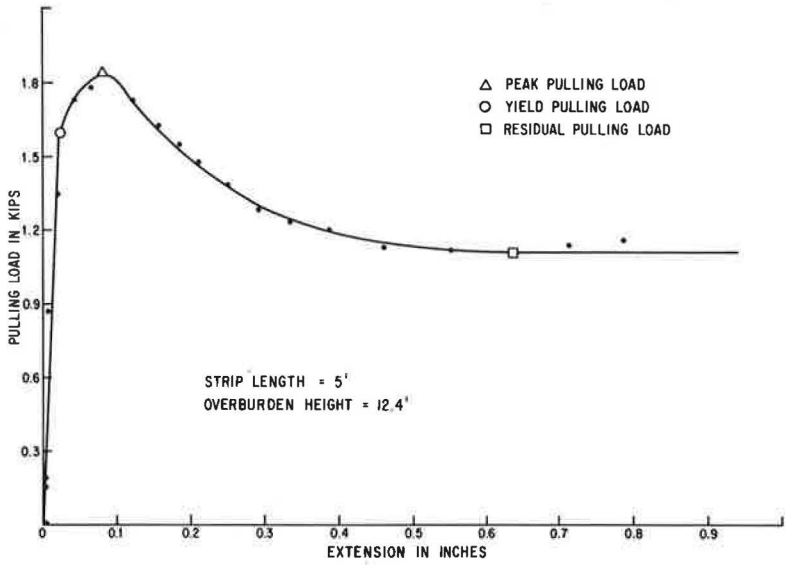

Figure 11. Residual pulling load, overburden load, overburden height, and strip length relationship.

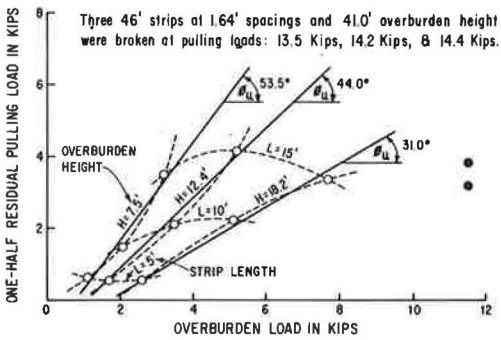

Figure 12. Overburden height, strip length, and slipping factor safety relationship.

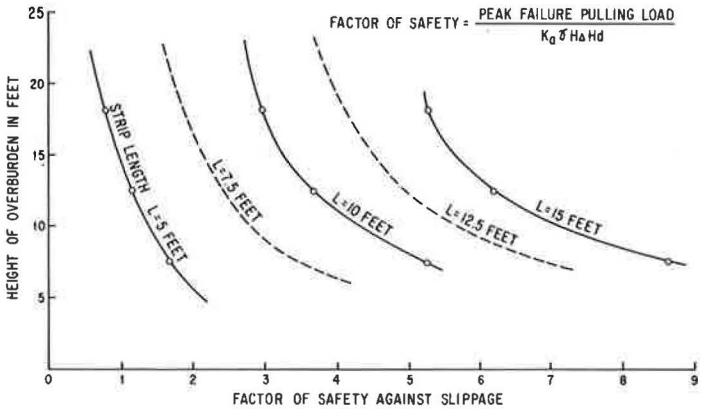

Figure 13. Relationship between pull load and skin-friction force.

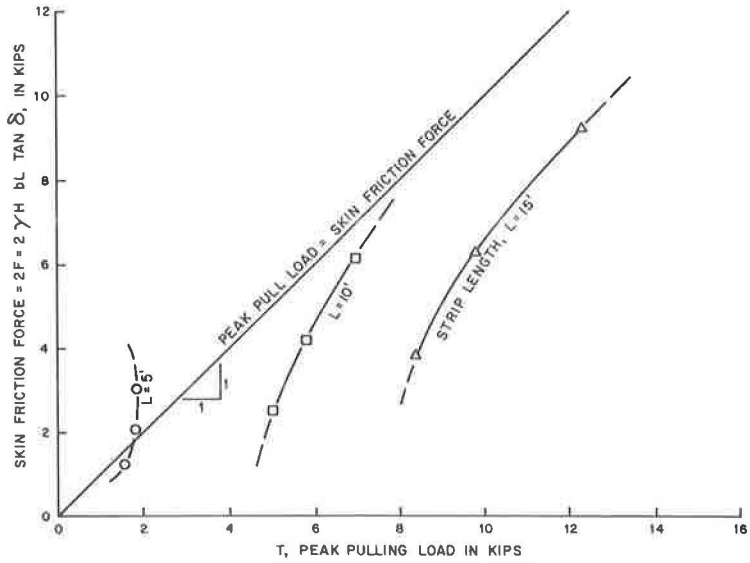

Figure 14. Relationship between overburden height and axial force in steel strip.

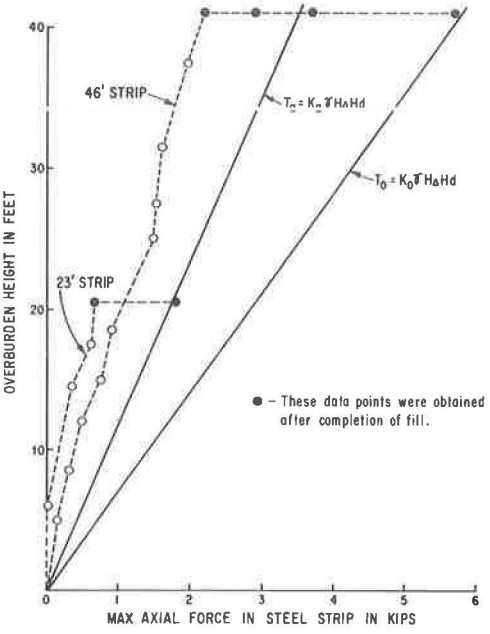

were highest during the early stages of construction and later decreased with large variations from point to point after completion of the fill.

The measured stresses in the steel strips near the wall face were generally smaller than, but approached, the calculated theoretical stresses, σ_a, based on Rankine's active stress condition. The highest steel stresses developed in the inner middle portion of the reinforced earth section. Steel stresses may increase to the values corresponding to theoretical at rest earth pressure. Equation 1, presented in this paper for the design of reinforcing strips, has been verified. The use of the active earth pressure coefficient, K_a, for calculating the steel stress is applicable for the end portion of the reinforcements. For the middle portion of the reinforcement, K_o should be used.

Field pulling test results indicated that the load-deformation curves resembled the stress-strain curves obtained from laboratory triaxial compression tests on dense sand when the strips were pulled loose. The yielding, peak, and residual load points were all defined clearly. The frictional forces developed on the steel strips were proportional to the overburden load for each overburden height. The field-measured skin-friction angle agreed well with the laboratory test results under equal overburden height. The relationships between the overburden height, strip length, and the factor of safety against slippage as shown in Figure 12 can be used for determining the minimum length of reinforcement for different overburden height, providing the requirement for stability is met. However, strip length should be at least 10 ft.

The structural behavior of the skin plates followed the hinged-end assumption in deformed shape and stress values. The vertical deformation of the skin plate, which is a measurement of settlement within each skin element, was proportional to the overburden height. Design Eq. 5, developed in this paper for design of the steel skin plate, accurately predicted the stresses developed in the skin plate. Use of the vertical deformation, δ_v, of the skin plate for one of the major functions in design has proven to be a satisfactory approach. Figure 9(b) can be used to estimate the vertical deformation, δ_v, for design of skin plate at different heights of reinforced earth fill. The assumption of a semicircular shape simplified the calculation of the stresses in the skin plate and accurately predicted the measured stresses.

The settlement and horizontal movement of the reinforced earth embankment was primarily attributable to the densification of the deep foundation slide debris. These movements were probably the main cause of continuing change in stresses of the steel and soil after completion of the fill.

ACKNOWLEDGMENTS

This paper presents the results of a federally financed research project. The writers wish to acknowledge and thank Gary Bork and John Kenan who were in charge of overall project design. The patience and cooperation of Robert F. Britton, who provided valuable assistance in installing the instrumentation during construction, also are gratefully acknowledged. This work was done under the HPR Work Program in cooperation with the Federal Highway Administration. The contents of this paper reflect the views of the authors, who are responsible for the facts and the accuracy of the data presented herein. The contents do not necessarily reflect the official views or policies of the State of California or the Federal Highway Administration.

REFERENCES

1. Duncan, W. Caesar. Vol. 1, Book 2, p. 201.
2. Vidal, H. The Principle of Reinforced Earth. Highway Research Record 282, 1969, pp. 1-16.
3. Chang, J. C., Forsyth, R. A., and Smith, T. W. Reinforced Earth Highway Embankment—Road 39. Highway Focus, Federal Highway Admin., Vol. 4, No. 1, Jan. 1972.
4. Chang, J. C., Durr, D. L., and Forsyth, R. A. Earthwork Reinforced Techniques. Transportation Lab., California Department of Transportation, TL No. 632115, Feb. 1974.

5. Seely, F. B., and Smith, J. O. Advanced Mechanics of Materials. John Wiley and Sons, Inc., New York, July 1962, pp. 421-437.
6. Jaky, J. Pressure in Silos. Proc. 1st Conf. on Soil Mech. and Found. Engineering, Rotterdam, 1948.